Transverse Fracture of Brittle Bilayers: Relevance to Failure of All-Ceramic Dental Crowns

Jae-Won Kim, Sanjit Bhowmick, Ilja Hermann, Brian R. Lawn

Materials Science and Engineering Laboratory, National Institute of Standards and Technology, Gaithersburg, Maryland 20899-8500

Abstract: This study examines the behavior of cracks approaching interfaces in all-ceramic dental crown-like bilayers. Flat specimens are fabricated by fusing porcelain veneers onto yttria-tetragonal-zirconia-polycrystal (Y-TZP) and alumina core ceramic plates, with veneer/core matching to minimize residual thermal expansion mismatch stresses. Vickers indentations are placed on either side of the interfaces, at systematically decreasing distances, so that the lead corner cracks approach and intersect the interfaces in a normal orientation. Cracks originating in the porcelain arrest at the boundaries and, after further diminution in indentation distance, deflect along the interface without penetration into the tough core ceramic. Cracks initiating in the core ceramic pass unimpeded into the weaker porcelain without deflection, and with abrupt increase in crack size. These latter cracks, because of their lack of containment within the core layer, are regarded as especially dangerous. Implications concerning the design of optimal dental crowns in relation to materials optimization are considered. © 2006 Wiley Periodicals, Inc. J Biomed Mater Res Part B: Appl Biomater 79B: 58–65, 2006

Keywords: dental crowns; fracture modes; penetrating cracks; deflecting cracks; interfaces

INTRODUCTION

The stability of cracks near interfaces in brittle layer structures is relevant to the integrity of a variety of engineering applications.[1] It is especially pertinent to the performance of all-ceramic dental crowns in occlusal contact,[2–4] where various competing fracture modes—propagating downward from the top surface in weak veneer porcelain layers and upward from the lower surface in strong alumina or zirconia core support layers—have the potential to cause failure. Figure 1 depicts a variety of cracks that have been observed, some initiating at the veneer top surface and others from the core bottom surface.[5,6] The question arises as to what happens when such cracks approach and intersect the interface: arrest, deflect, or penetrate? Most work in the engineering fracture community has focused on the role of crack deflection along weak interfaces,[1,7,8] in the interest of imparting energy absorption or toughness to the structure. However, delamination is not an option in biomechanical structures such as dental crowns, and so great effort is generally made to construct material systems with adequately tough veneer/core interfaces. This transfers attention to interlayer crack

penetration. Clearly, penetration is no less undesirable than delamination, so it is important to understand the basic material properties that govern the resistance to this mode. In dental practice, the often complex and multimodal failures observed in all-ceramic dental crowns are not easily analyzed by postmortem examination,[9–14] so *in situ* tests on model layer structures offer the best insight into underlying mechanisms.

In this paper we describe some simple fracture experiments on flat bilayer structures that may be considered indicative of the damage resistance of all-ceramic dental crowns. For this purpose, dental porcelain veneering layers are fused onto flat yttria-tetragonal-zirconia-polycrystal (Y-TZP) or alumina core plates, with matched coefficient of thermal expansion (CTE). Vickers indentations are used to position cracks on polished cross sections, at prescribed loads and prescribed distances from the bilayer interfaces, in a manner described in an earlier study on other kinds of ceramic bilayers.[15] Indentation experiments of this kind have been used to probe interface fracture properties of bonded silicon wafers,[16] ceramic fiber-composite systems,[17] and dento-enamel junction interfaces in natural teeth,[18,19] among other material systems. In our specimens, corner radial cracks initiating in the tough core ceramic are found to pass readily into the porcelain veneer layer. Cracks initiating in the veneer tend to arrest and deflect at the interface. From these observations it is concluded that
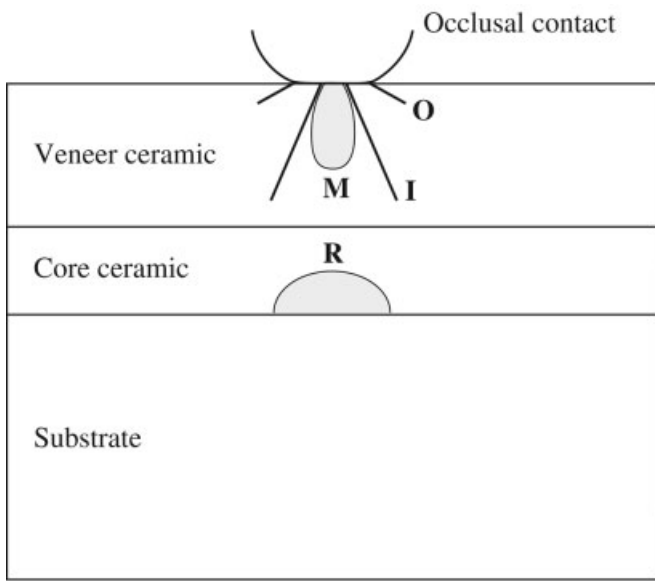
Figure 1. Schematic of crack geometry for cyclic contact on all-ceramic veneer/core bilayer bonded onto compliant support base, showing a variety of crack modes produced by contact with sphere. Cracks originating from veneer top surface (Hertzian cone crack **O**, inner cone crack **I**, median crack **M**) or bottom surface (radial crack **R**) can intersect veneer/core interface and either arrest, penetrate, or deflect.[5,6]

core fractures, when they do occur, represent the greater threat to through-thickness failure of crowns.

EXPERIMENT

The bulk of the experiments were carried out using dental porcelains as the top (veneer) ceramic layer, and stiff, tough zirconia and alumina as the bottom (core) ceramic layer. Material properties are listed in Table I. The core materials were Y-TZP (Prozyr Y-TZP, Norton, East Granby, CT) and alumina (AD995, CoorsTek, Golden, CO), provided as plates $25 \times 25 \times 1$ mm^3. Prospective joining surfaces were polished to 1 μm finish, to provide well-defined interfaces. In accordance with dental practice, the porcelains were chosen to provide a CTE match with the core material (differential $<$ 0.5×10^{-6} °C^{-1}): IPS d.SIGN (Ivoclar–Vivadent, Schaan, Liechtenstein) on Y-TZP; and Vitadur Alpha (Vita Zahnfabrik, Bad Sackingen, Germany) on alumina. The porcelains were applied in layers, with sequential firings, to a final thickness $\approx$ 1 mm. Sections were cut normal to the internal

TABLE I. Parameters for Materials in This Study

Material	E (GPa)	T (MPa m$^{1/2}$)	R (J m^{-2})[a]
Y-TZP	205	7.2	240
Al$_2$O$_3$	370	2.5	16
Porcelain	65	0.65	6.2

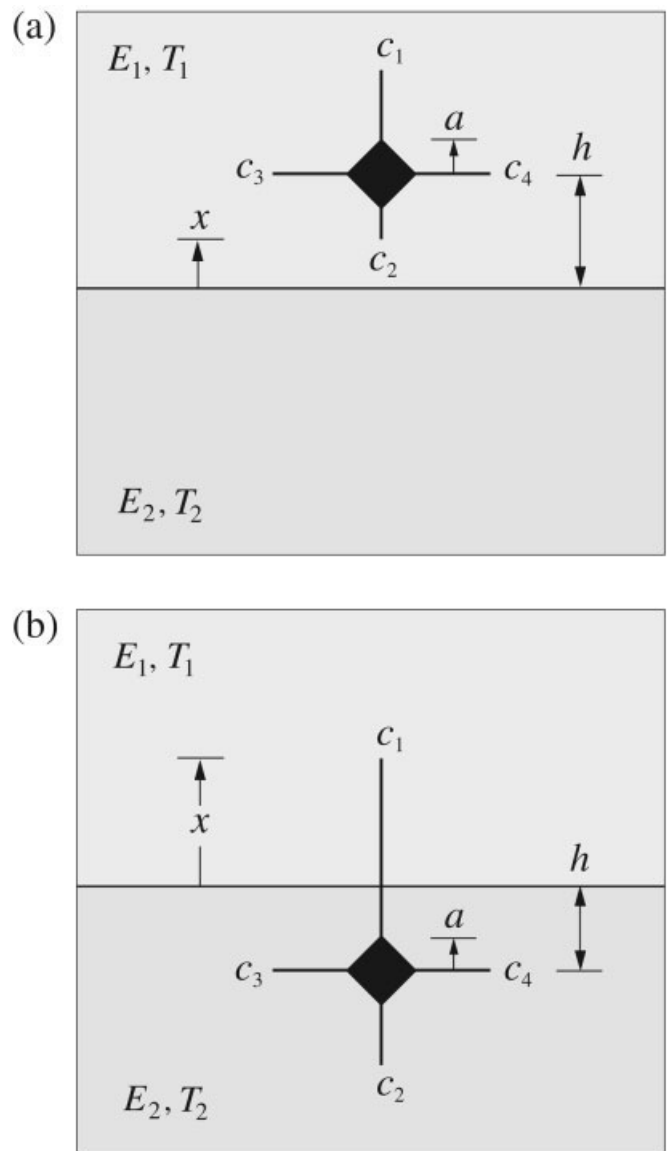[a] R calculated using common Poisson's ratio $\nu = 0.22$.

Figure 2. Coordinates of Vickers crack system traversing interface, showing cracks from indentations in (a) veneer (layer 1) and (b) core (layer 2). Indentation center distance h from interface and half-diagonal a. Corner crack arms c_1, c_2, c_3, and c_4 are measured from indentation center, x designates distance between lead crack tip and interface.

interface and polished down to 1 μm finish. No indication of delamination was found during fabrication of these specimens.

Vickers indentations were placed in the specimen sections at prescribed distances from the veneer/core interface, at loads 10 N in the porcelains and alumina and 40 N in the Y-TZP. (The larger load in the last case was to maintain well-defined corner radial cracks at the indentation corners.) The indentations were carefully aligned with the corner cracks perpendicular and parallel to the interface, as in Figure 2. The indented surfaces were gold coated to improve crack visibility. Crack lengths c_1, c_2, c_3, and c_4 from the indentation centers were measured as a function of indentation distance h from the interface by optical microscopy.
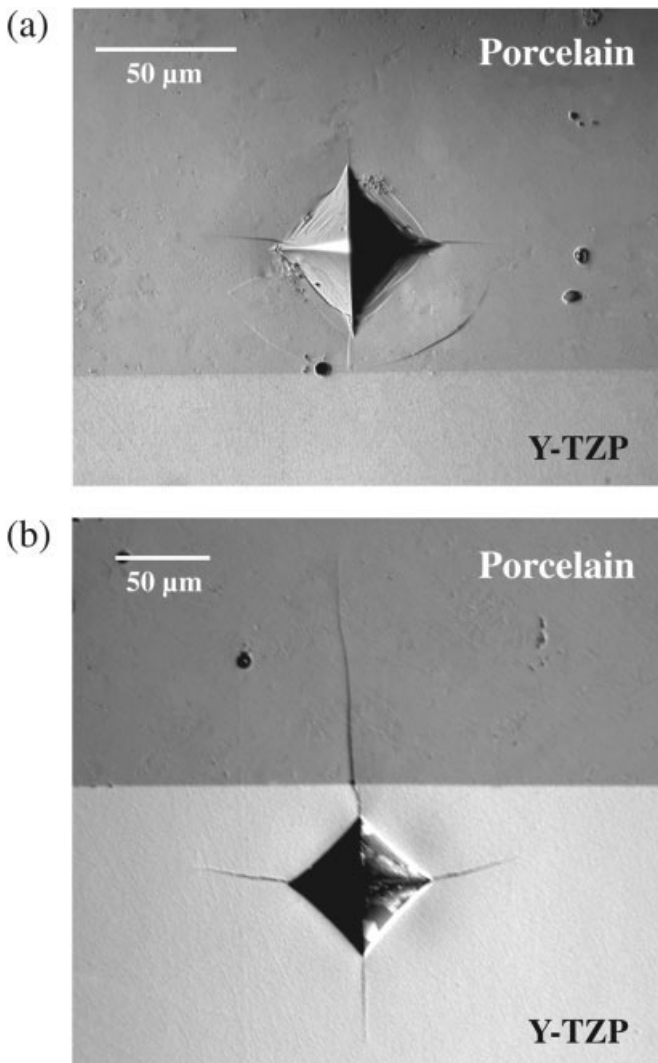
Figure 3. Cracks from Vickers indentations in porcelain/Y-TZP bilayer. Indentations in (a) porcelain, (b) Y-TZP. Note arrest of crack at interface in (a), enhanced penetration across interface in (b).

A few secondary experiments using various silicate glass plates bonded to Y-TZP were also conducted, to examine the effect of larger CTE mismatch. In this case the glass plates were fused onto the bottom layer with glass tape (G-1001 transfer tape, Vitta Corp, Bethel, CT) at 600°C for 30 min, and then refired at 800°C for 20 min with the top surface in place. The final tape thickness was ≈50 μm. In these specimens crack analyses were restricted to qualitative observations.

CRACK MEASUREMENTS

Micrographs of Vickers cracks in the porcelain-based layer specimens are shown in the micrographs of Figures 3 and 4 for Y-TZP and alumina, respectively, for indentations located in (a) the veneering porcelain and (b) the ceramic core layer. In neither ceramic-core system do lead cracks originating in

the porcelain [c_2 in Figure 2(a)] penetrate into the adjacent layer, first arresting [Figure 3(a)] and subsequently deflecting [Figure 4(a)] at the interface. (Note the appearance of an arc-like lateral crack at the bottom of the porcelain layer in Figure 3(a)—these cracks are commonly observed in glass surfaces, especially near interfaces or edges, and do not impede the radial crack.[20]) Conversely, lead cracks originating in the Y-TZP [Figure 3(b)] and alumina [Figure 4(b)] layers [c_1 in Figure 2(b)] penetrate abruptly and extend substantially in length into the porcelain. The laterally extending corner cracks [c_3 and c_4 in Figure 2(b)] in the core ceramics bend toward the interface, the more so in the alumina [Figure 4(b)] where the elastic mismatch is greater, as if attracted by the compliant porcelain layer on the other side.[21] No deflection at the interface was observed for any core-originated cracks traversing the interface. All such cracks remained relatively steady with time, growing less than 5% in length over a week, indicating only minor influence of moisture-assisted crack growth within the residual elastic–plastic indentation stress field.[22]
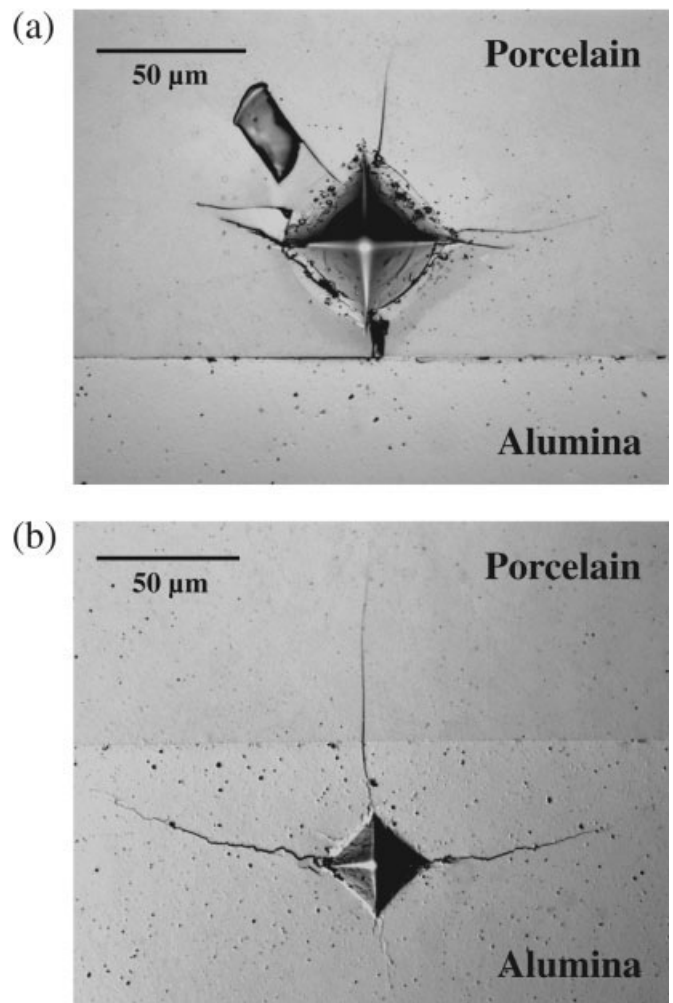

Figure 4. Cracks from Vickers indentations in porcelain/alumina bilayer. Indentations in (a) porcelain, (b) alumina. Note arrest of crack and delamination at interface in (a), penetration across interface in (b).

Figure 5. Crack sizes c_1, c_2, c_3, and c_4 *versus* distance h of indentation center to interface in porcelain/Y-TZP bilayers. Indentations in (a) porcelain and (b) Y-TZP, orientation relative to interface indicated by inset.

Measurements of crack size as a function of distance h of the indentation center from the interface (Figure 2) are plotted in Figure 5 for porcelain/Y-TZP and Figure 6 for porcelain/alumina. Data at large h tend to a common asymptotic limit, $c_1 = c_2 = c_3 = c_4 = c_0$ (say), in accordance with the absence of significant residual CTE stresses. The largest influence of the elastic mismatch is felt by the lead cracks, c_2 in Figures 5(a) and 6(a) and c_1 in Figures 5(b) and 6(b). Note the distinct jump in the c_1 data at small h in Figure 5(b) [somewhat less pronounced in Figure 6(b)], corresponding to cracks that have intersected the interface (i.e. $c_1 > h$) and penetrated into the less tough porcelain. (These data are limited by the requirement that $h > a$ in Figure 2, in order that there be a well-defined lead crack.) Conversely, the decline in the c_2 data at small h in Figures 5(a) and 6(a) signifies crack arrest or deflection at the interface. The smallest influence of mismatch is felt by the more remote cracks, c_1 in Figures 5(a) and 6(a) and c_2 in Figures 5(b) and 6(b). As expected by symmetry, c_3 and c_4 for the laterally extending arms are mutually indistinguishable within the data scatter at all h.

ANALYSIS

Following an approach used in an earlier paper,[15] we begin by writing a stress-intensity factor for Vickers corner radial cracks in a homogeneous material

$$K_0 = \chi P / c^{3/2} \qquad (1)$$

where $\chi = \zeta (E/H)^{1/2}$ is an elastic–plastic coefficient,[23] with E the modulus and H the hardness of the material containing the indentation impression and ζ is a material-independent coefficient. Plots of K_0 as a function of crack coordinate x (Figure 2) are given in Figures 7 and 8 for porcelain/Y-TZP and porcelain/alumina, respectively. Coordinate x is the distance between lead crack tip and interface, i.e. $x = h - c_2$ for indentations in the porcelain veneer layer [Figures 7(a) and 8(a)] and $x = c_1 - h$ for indentations in the Y-TZP or alumina core layer [Figures 7(b) and 8(b)]. In this coordinate system, $x = 0$ corresponds to intersection of the crack tip with the interface.
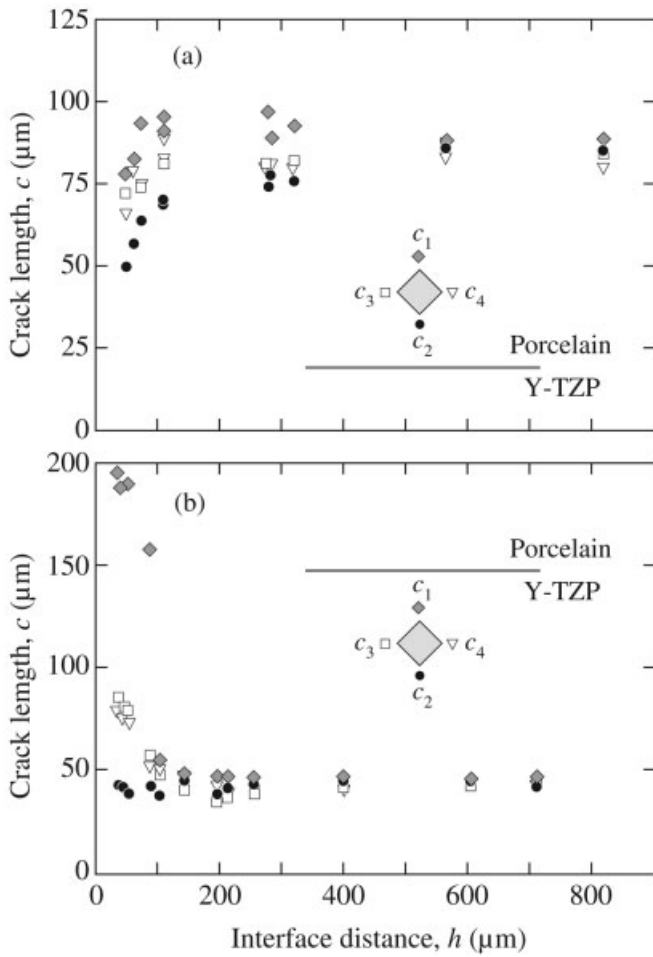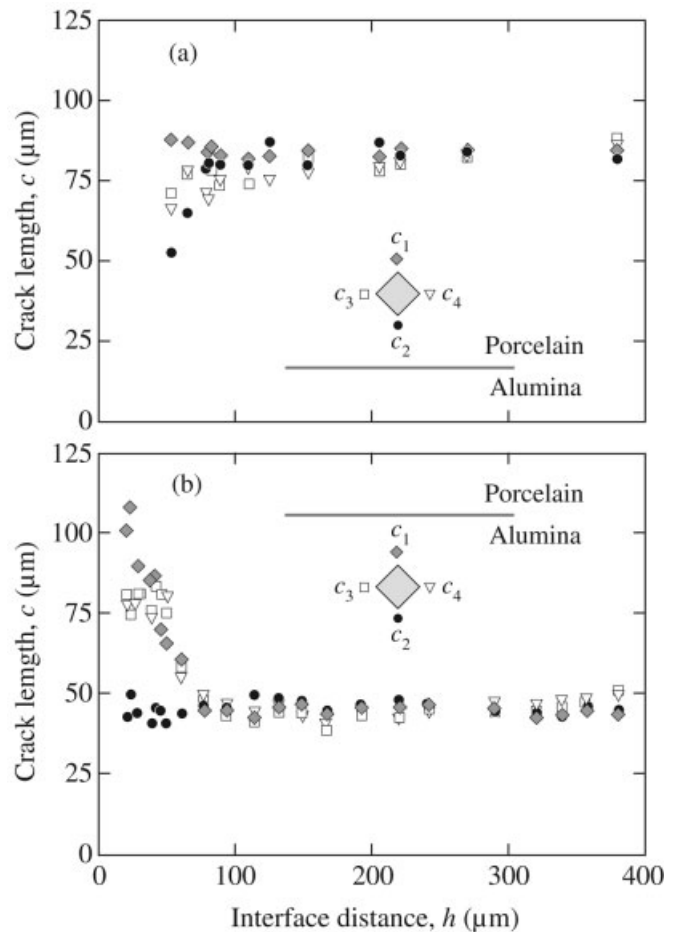

Figure 6. Crack sizes c_1, c_2, c_3 and c_4, *versus* distance h of indentation center to interface in porcelain/alumina bilayers. Indentations in (a) porcelain and (b) alumina, orientation relative to interface indicated by inset.
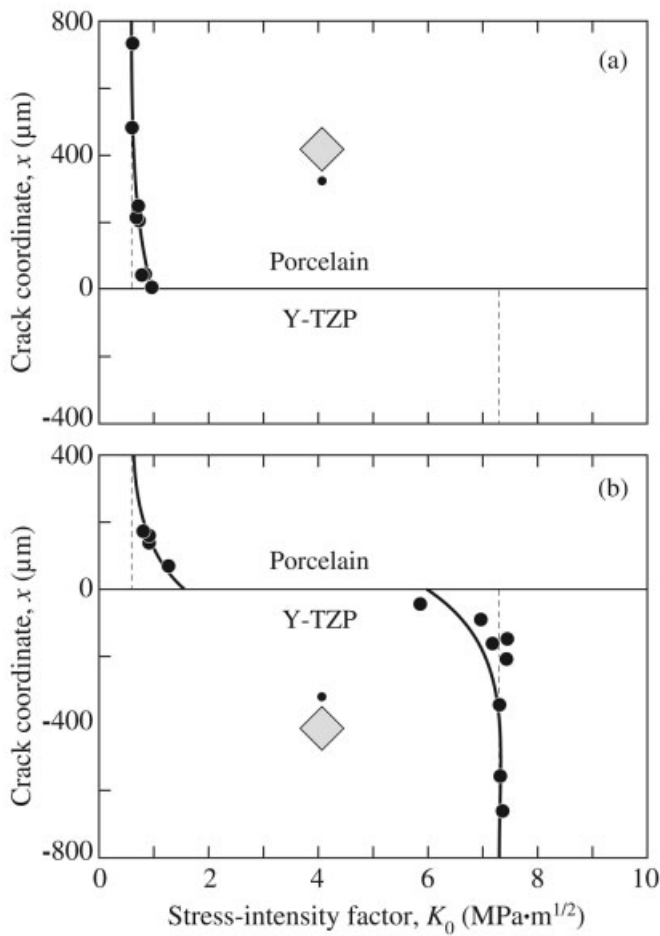
Figure 7. Stress-intensity factor K_0 (horizontal axis) *versus* distance $x = c - h$ of lead crack tip from interface (vertical axis), for porcelain/Y-TZP bilayers. Indentations in (a) porcelain, (b) Y-TZP, as indicated by inset. Solid lines are empirical fits to the data, dashed vertical lines are asymptotic toughness T bounds.

It will be noted that the K_0 functions in Figures 7(b) and 8(b) include data for core cracks that have penetrated into the adjacent veneer layer. Moreover, K_0 in all of Figures 7 and 8 varies even when the crack is wholly contained in the originating material, indicating some influence of elastic mismatch.[21] Hence K_0 is not a true toughness. To allow for the influence of the bilayer properties, we write

$$K = \alpha K_0 \qquad (2)$$

where $\alpha = \alpha\,(x/h, E_1/E_2)$ is a dimensionless function. Then the condition for equilibrium crack extension is that $K = T$, where $T = K_{IC}$ is the toughness of the material containing the crack tip. For cracks with tips distant from the interface (i.e. $x \gg 0$ or $\ll 0$), α tends to unity, establishing useful asymptotic limits at T values (vertical dashed lines) listed in Table I. The solid curves in Figures 7 and 8 are empirical fits through the data, and provide a measure of α in Eq. (2).

Arguably the most interesting feature in Figures 7 and 8 are the functional discontinuities in the $K_0(x)$ functions at the

interface, associated with the abrupt changes in toughness and modulus. Consider what happens as the indentation is allowed to approach the interface, i.e. steadily decreasing h. For indentations in the veneer porcelain the lead corner crack will slow down as it approaches the interface and ultimately arrest there. The crack will then remain stationary as h continues to diminish, until K_0 reaches a sufficiently high level to cause either penetration or deflection. Conversely, for indentations in the core ceramic, the leading crack will accelerate as it approaches and intersects the interface, at which point it will jump abruptly into the porcelain (pop in). Continued decrease in h will cause the extended crack to penetrate further into the porcelain without interruption in the growth. Since they are not contained, cracks that initiate in the tougher and stiffer core ceramic would appear to pose the more immediate threat to integrity of the all-ceramic bilayer system.

This leaves the issue of crack penetration *versus* deflection. This issue has been addressed by He and Hutchinson.[24] Figure 9 is a plot of energy-release-rate G_i/G_b (subscript i
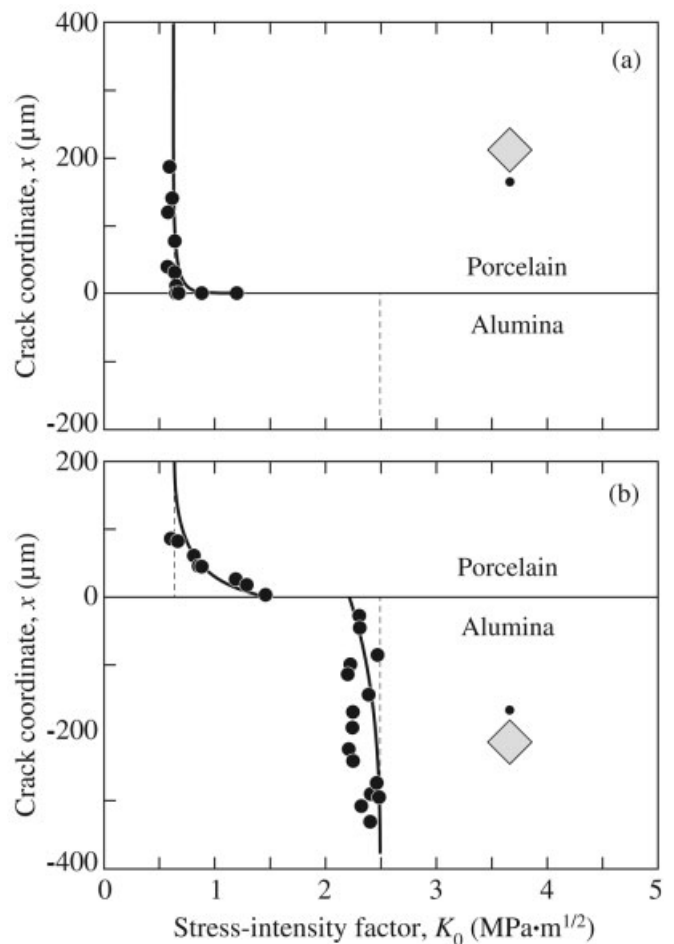

Figure 8. Stress-intensity factor K_0 (horizontal axis) *versus* distance $x = c - h$ of lead crack tip from interface (vertical axis), for porcelain/alumina bilayers. Indentations in (a) porcelain, (b) alumina, as indicated by inset. Solid lines are empirical fits to the data, dashed vertical lines are asymptotic toughness T bounds.
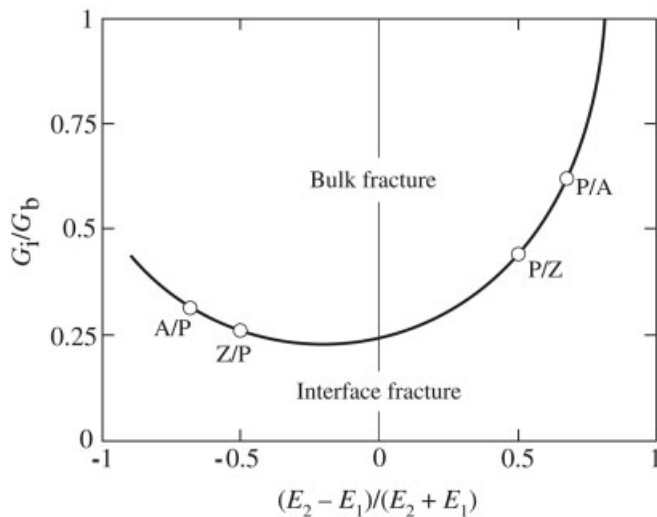
Figure 9. Plot of relative energy-release-rate G_i/G_b for crack deflection along interface relative to penetration into adjacent bulk material across interface. Points are critical values for cracks from porcelain to alumina (P/A), porcelain to Y-TZP (P/Z), Y-TZP to porcelain (Z/P), and alumina to porcelain (A/P).

referring to interface and b to bulk on far side of interface) *versus* modulus mismatch parameter $(E_2 - E_1)/(E_2 + E_1)$ for a singly-deflecting crack. Points P/A and P/Z on the curve indicate values of $(E_2 - E_1)/(E_2 + E_1)$ for veneer-to-core cracks, Z/P and A/P values for core-to-veneer cracks. Whether it is penetration or deflection that occurs first depends whether the crack resistance ratio R_i/R_b is greater or less than the appropriate critical G_i/G_b values in Figure 9, where $R_i = T_i^2(1 - \nu_i^2)/E_i$ and $R_b = T_b^2(1 - \nu_b^2)/E_b$ (with ν Poisson's ratio).[25] Values of R_i/R_b above the curve constitute the domain of crack penetration into the adjacent bulk layer, below the curve the domain of deflection along the interface. In our systems, cracks originating in the veneer porcelain always arrested, and later deflected, at the interface [Figures 3(a) and 4(a)]. Cracks originating in the core ceramic always penetrated into the adjacent bulk layer. These observations, in combination with the critical G_i/G_b values in Figure 9 and crack resistance energies R_b for the bulk materials included in Table I, enable us to establish upper and lower bounds to R_i for the two systems: for the Y-TZP core bilayers, 1.6 J m^{-2} $\leq R_i \leq 105$ J m^{-2}; for the alumina core bilayers, 2.0 J m^{-2} $\leq R_i \leq 9.9$ J m^{-2}.

DISCUSSION

In this paper we have used Vickers indentation cracks to probe the behavior of cracks intersecting interfaces in all-ceramic bilayers, porcelain bonded to either Y-TZP or alumina. Specifically, we have observed crack paths and measured crack lengths as a function of indentation–interface distance. Lead cracks that initiate within the weak porcelain veneer layers arrest at the interface, ultimately spreading as a delamination crack as the indentation moves closer to the adjacent layer. Conversely, lead cracks that initiate in the tougher and stiffer core ceramic are increasingly attracted to the relatively compliant porcelain, and upon intersection with the interface, penetrate and extend abruptly in length into the porcelain. The results confirm the significant influence of elastic and toughness mismatch of the bilayer members and highlight the susceptibility of the weak porcelain to damage originating on both sides.

The competition between penetration and deflection provides bounding estimates of interface energies. In our cases, values in excess of 1 J m^{-2} were measured between porcelain veneers and ceramic core layers, indicative of moderate chemical bonding. Such levels are sufficient to prevent the interfaces from delaminating when cracks traverse from the core to the porcelain (although not vice versa). (More explicit estimates of interface energies have been obtained in some systems by inclining the cracks in the core ceramic layers relative to the interface, and determining the critical angle at which the mode changes from penetration to deflection.[26]) Lesser bonding, e.g. interfacial joining by epoxy adhesive, will inevitably tilt the balance away from penetration toward delamination, a fact exploited in the design of ultra-tough multilayers for crack containment.[8] It is apparent that knowledge of interface energies relative to the bulk is a vital ingredient in the performance of ceramic layer systems, especially in biomechanical applications where delaminations are hardly an option.

Another factor that warrants consideration is the role of residual stress from thermal expansion mismatch during the bilayer fabrication. In our experiments we have avoided this issue, in accordance with dental practice, by choosing porcelains that closely match the CTE of the adjoining core ceramics. However, such stresses could become an important factor in some systems. As an illustrative example, we show in Figure 10 a photograph of a Vickers indentation in Y-TZP bonded to borosilicate glass at 800°C, taken a week after indentation. In this case the CTE mismatch is $\alpha = \alpha_{Y\text{-}TZP} - \alpha_{glass} \approx 5 \times 10^{-6}$ °C^{-1}, which can give rise to tensile stresses > 150 MPa in the Y-TZP.[27] Slow crack growth has resulted in spontaneous failure of the specimen. Note how the crack has run directly across the specimen in the tensile Y-TZP and bent around toward a near-parallel orientation in the compressive glass.[28] The design of layer structures with CTE mismatch stresses clearly needs to be undertaken with due caution.

Finally, some comments on the clinical relevance of our results are in order. Dental crowns are subjected to concentrated loading from occlusal contact at the veneer top surface. The porcelain veneer layer is typically compliant but weak, the ceramic core layer stiff and strong. On the face of it, the current results suggest that cracks originating from the veneer top surface are likely to be arrested, or at worst deflected, at the interface. This suggestion is borne out in experiments on glass/alumina/polycarbonate trilayers using loading geometries of the kind depicted in Figure 1.[29] Cracks originating from the core lower surface, how-
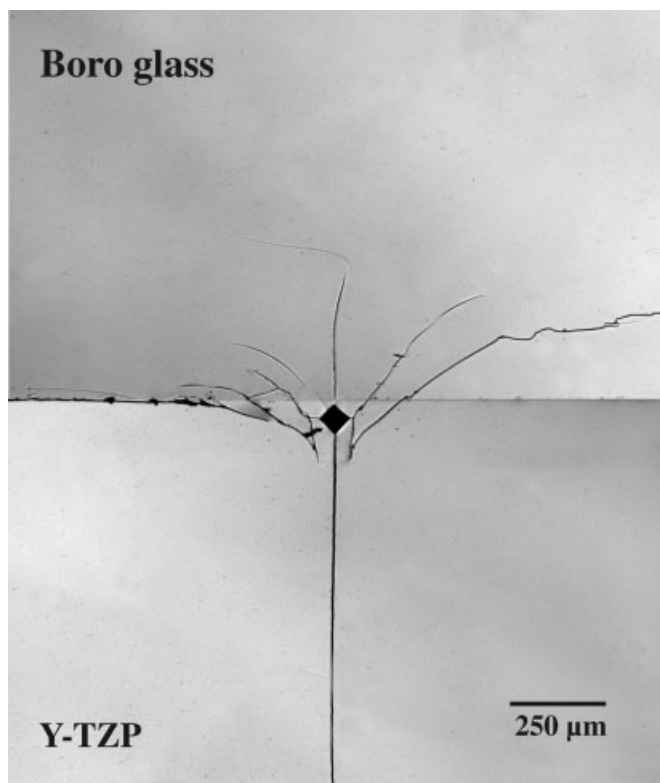
Figure 10. Cracks from Vickers indentations in borosilicate-glass/glass-tape/Y-TZP trilayer, showing crack penetration from Y-TZP into glass, 1 week after indentation. Note crack runs directly through in Y-TZP layer, consistent with tensile state, but bends around toward near-parallel orientation in glass, consistent with compressive state.

ever, are likely to penetrate unimpeded into the veneer. The latter cracks would appear to be especially dangerous because they may (especially at high contact load or in cyclic loading) propagate to the top surface of the crown,[30] exposing the cementation surface to the oral environment. In such contact loading the layers are subject to superposed flexural as well as contact stresses.[31] These flexural stresses could play an important role in determining the ultimate propagation of transverse cracks through the thickness. For low-modulus veneers on high-modulus cores in particular, much of the load from bilayer flexure is transferred to the stiffer core layer, enhancing tension in that layer and suppressing it in the veneer.[31,32] Such a stress redistribution will tend to counteract the low toughness of the veneer, somewhat inhibiting crack penetration from the core to the top surface. Further study of these more complex stress effects as they relate to crown structures, including the potentially exacerbating role of specimen curvature on failure conditions,[33] would appear to be warranted.

REFERENCES

1. Hutchinson JW, Suo Z. Mixed-mode cracking in layered structures. Adv Appl Mech 1992;29:63–191.

2. Kelly JR, Giordano R, Pober R, Cima MJ. Fracture surface analysis of dental ceramics: Clinically failed restorations. Int J Prosthodont 1990;3:430–440.

3. Kelly JR. Ceramics in restorative and prosthetic dentistry. Annu Rev Mater Sci 1997;27:443–468.

4. Kelly JR. Clinically relevant approach to failure testing of all-ceramic restorations. J Prosthet Dent 1999;81:652–661.

5. Lawn BR, Deng Y, Thompson VP. Use of contact testing in the characterization and design of all-ceramic crown-like layer structures: A review. J Prosthet Dent 2001;86:495–510.

6. Lawn BR, Pajares A, Zhang Y, Deng Y, Polack M, Lloyd IK, Rekow ED, Thompson VP. Materials design in the performance of all-ceramic crowns. Biomaterials 2004;25:2885–2892.

7. Cook J, Gordon JE. A mechanism for the control of crack propagation in all-brittle systems. Proc R Soc Lond 1964;A282:508–520.

8. Clegg WJ, Kendall K, Alford NM, Button TW, Birchall JD. A simple way to make tough ceramics. Nature 1991;347:455–457.

9. Fradeani M, Aquilano A. Clinical experience with empress crowns. Int J Prosthodont 1997;10:241–247.

10. Oden A, Andersson M, Krystek-Ondracek I, Magnusson D. Five-year clinical evaluation of procera allceram crowns. J Prosthet Dent 1998;80:450–456.

11. Malament KA, Socransky SS. Survival of dicor glass-ceramic dental restorations over 14 years: I. Survival of dicor complete coverage restorations and effect of internal surface acid etching, tooth position, gender and age. J Prosthet Dent 1999;81:23–32.

12. Sjogren G, Lantto R, Tillberg A. Clinical evaluation of all-ceramic crowns (dicor) in general practice. J Prosthet Dent 1999;81:277–284.

13. Sjogren G, Lantto R, Granberg A, Sundstrom BO, Tillberg A. Clinical examination of leucite-reinforced glass-ceramic crowns (empress) in general practice: A retrospective study. Int J Prosthodont 1999;12:122–128.

14. McLaren EA, White SN. Survival of in-ceram crowns in a private practice: A prospective clinical trial. J Prosthet Dent 2000;83:216–222.

15. Wuttiphan S, Lawn BR, Padture NP. Crack suppression in strongly-bonded homogeneous/heterogeneous laminates: A study on glass/glass–ceramic bilayers. J Am Ceram Soc 1996;79:634–640.

16. Latella BA, Nicholls TW, Cassidy DJ, Barbé CJ, Triani G. Evaluation of interfacial toughness and bond strength of sandwiched silicon structures. Thin Solid Films 2002;411:247–255.

17. Morgan PED, Marshall DB. Ceramic composites of monazite and alumina. J Am Ceram Soc 1995;78:1553–1563.

18. Xu HHK, Smith DT, Jahanmir S, Romberg E, Kelly JR, Thompson VP. Indentation damage and mechanical properties of human enamel and dentin. J Dent Res 1998;77:472–480.

19. Imbeni V, Kruzic JJ, Marshall GW, Marshall SJ, Ritchie RO. The dentin–enamel junction and the fracture of human teeth. Nat Mater 2005;4:229–232.

20. Burghard Z, Zimmermann A, Rödel J, Aldinger F, Lawn BR. Crack opening profiles of indentation cracks in normal and anomalous glasses. Acta Mater 2004;52:293–297.

21. Lardner TJ, Ritter JE, Shiao ML, Lin MR. Behavior of indentation cracks near free surfaces and interfaces. Int J Fract 1990;44:133–143.

22. Lawn BR, Jakus K, Gonzalez AC. Sharp vs. blunt crack hypotheses in the strength of glass: A critical study using indentation flaws. J Am Ceram Soc 1985;68:25–34.

23. Lawn BR, Evans AG, Marshall DB. Elastic/plastic indentation damage in ceramics: The median/radial crack system. J Am Ceram Soc 1980;63:574–581.

24. He M-W, Hutchinson JW. Crack deflection at an interface between dissimilar elastic materials. Int J Solids Struct 1989;25:1053–1067.

25. Lawn BR. Fracture of Brittle Solids. Cambridge: Cambridge University Press; 1993, Ch 2.

26. Becher PF, Hwang SL, Lin HT, Tiegs TN. Microstructural contributions to the fracture resistance of silicon nitride ceramics. In: Hoffmann MJ, Petzow G, editor. Tailoring of Mechanical Properties of Si_3N_4. Dordrecht: Kluwer; 1994. p 87–100.

27. Wang H, Hu XZ. Surface properties of ceramic laminates fabricated by die pressing. J Am Ceram Soc 1996;79:553–556.

28. Sbaizero O, Lucchini E. Influence of residual stresses on the mechanical properties of a layered ceramic composite. J Eur Ceram Soc 1996;16:813–818.

29. Hermann I, Bhowmick S, Zhang Y, Lawn BR. Competing fracture modes in brittle materials subject to concentrated cyclic loading in liquid environments: Trilayer structures. J Mater Res. In press.

30. Rudas M, Qasim T, Bush MB, Lawn BR. Failure of curved brittle layer systems from radial cracking in concentrated loading. J Mater Res 2005;20:2812–2819.

31. Miranda P, Pajares A, Guiberteau F, Cumbrera FL, Lawn BR. Contact fracture of brittle bilayer coatings on soft substrates. J Mater Res 2001;16:115–126.

32. Taskonak B, Mecholsky JJ, Anusavice KJ. Residual stresses in bilayer dental ceramics. Biomaterials 2005;26:3235–3241.

33. Qasim T, Bush MB, Hu X, Lawn BR. Contact damage in brittle coating layers: Influence of surface curvature. J Biomed Mater Res 2005;73B:179–185.